Binary Mixtures of Proton-conducting Ionic Liquids as Electrolytes for Medium-Temperature Polymer Electrolyte Membrane Fuel Cells

Yanpeng Suo,[1, 2] Hui Hou,[1, 2] Jingjing Lin,[1, 2] Yingzhen Chen,[1, 2] Chang Liu,[1, 3] Ce Wang,[4] Peter S. Schulz,[5] Klaus Wippermann,[1] and Carsten Korte[1, 2]*

[1] Forschungszentrum Jülich GmbH, Institute of Energy and Climate Research – Electrochemical Process Engineering (IEK-14), Wilhelm-Johnen-Straße, 52425 Jülich, Germany

[2] RWTH Aachen University, 52062 Aachen, Germany

[3] Modeling in Electrochemical Process Engineering, RWTH Aachen University, 52056 Aachen, Germany

[4] FH Aachen Campus Jülich, 52428 Jülich, Germany

[5] Institute of Chemical Reaction Engineering, Friedrich-Alexander University Erlangen–Nürnberg, 91058 Erlangen, Germany

*corresponding author; tel.: +49 2461 61 2572; fax: +49 2461 61 6695; e-mail address: k.wippermann@fz-juelich.de

Keywords: fuel cell, proton-conducting ionic liquids (PILs), PIL blends, ORR kinetics.

Abstract

In this study, a physico-chemical and electrochemical characterization of mixtures of proton- conducting ionic liquids (PILs) is reported for on for potential future use as a novel electrolyte in polymer electrolyte membrane fuel cells (PEMFCs), operable at 100–120 °C. By blending two PILs, 2-Sulfoehyl-methyl-ammonium triflate [2-Sema][TfO] and Diethyl-methyl-ammonium triflate [Dema][TfO], exhibiting different cation acidities and different oxygen diffusivities/solubilities, it was apparent that the superior physico-chemical and electrochemical properties of both PILs can be favorably combined. Improved thermal stability of the blend, compared to neat [2-Sema][TfO], was observed. The viscosity of the mixtures decreased when increasing the fraction of [Dema][TfO], which led to increased proton conductivity and oxygen transmission coefficients, *i.e.*, $D_{O_2} \cdot c_{O_2}$. In combination with the highly acidic [2-Sema]$^+$ cations, which served as strong proton donors for the oxygen reduction reaction (ORR), the latter led to an increase in the ORR limiting current density at cell potentials relevant for fuel cell operation.

1. Introduction

Ionic liquids (ILs) are salts with bulky cations and anions, a low lattice energy and so a melting point below 100 °C, or even below room temperature.[1] An important class of ILs are proton-conducting ionic liquids (PILs), which also have essentially similar properties to aprotic ionic liquids (AILs), *e.g.*, high thermal and chemical stabilities, low flammability, low vapor pressure, high ionic conductivity, and a wide electrochemical window.[2, 3] The superior properties of PILs have attracted growing interest for their application in fuel cells.[4]

As non-aqueous proton-conductors, PILs may be promising electrolytes for medium-temperature polymer electrolyte membrane fuel cells (MT-PEMFCs), which operate at 100–120 °C.[5] Wippermann et al.[4] reported the electrochemical properties of the highly acidic PIL 2-Sulfoethyl-ammonium triflate [2-Sea][TfO] for use as an electrolyte in PEMFCs. It exhibits improved oxygen reduction reaction (ORR)

kinetics compared to phosphoric acid (H_3PO_4), and is used as an electrolyte in high-temperature (HT-)PEFCs. H_3PO_4 species are adsorbed on the catalyst surface, leading to the blockage of ORR-active sites and the PIL cations and triflate anions not interacting as strongly.

However, [2-Sea][TfO] has a very high viscosity due to a distinct tendency to form interionic hydrogen bonds. The N-methylated derivate, 2-Sulfoethyl-methyl-ammonium triflate [2-Sema][TfO] exhibits only a slightly lower viscosity, *i.e.*, 0.22 Pa s at 90 °C. This value is very high compared to the viscosity of other, low-acidic PILs such as Diethyl-methyl-ammonium triflate [Dema][TfO] (0.01 Pa s at 90 °C). Due to the strong coupling of ionic/molecular transport and viscous flow, this leads, in the case of a vehicular mechanism, to a low specific ionic conductivity of 2.5 mS cm^{-1} and low O_2 diffusion coefficient D_{O_2} of $2.48 \cdot 10^{-6}$ cm^2 s^{-1} at 90 °C for [2-Sema][TfO].[6] Due to its strong polar/hydrophilic properties, the O_2 solubility c_{O_2} is also low. Both are crucial parameters for the ORR kinetics. These drawbacks would limit the application of [2-Sema][TfO] as a PEFC electrolyte. Lee et al. first reported on the use of low-acidic PIL [Dema][TfO] as a fuel cell electrolyte.[7] Due to its low viscosity, [Dema][TfO] achieves a much higher specific ionic conductivity, *i.e.*, 10 mS cm^{-1} even at 30 °C.[8] It also achieves high values for D_{O_2} and c_{O_2} in a wide temperature range.[9] In own studies, it emerged that the ORR onset potential of the low-acidic [Dema][TfO] is very low, *i.e.*, 0.57 V *vs.* a Pd-H reference at 90 °C. In the case of the high-acidic [2-Sema][TfO], a much higher onset potential of 0.93 V *vs.* Pd-H is found. Only the latter matches the typical cathode potential range during a fuel cell operation of 0.8–1.0 V. In the case of non-aqueous electrolytes, the proton transfer also becomes rate-limiting for the ORR.[10] The low onset potential of [Dema][TfO] results in low current densities at application-relevant potentials.

The ΔpK_a of the corresponding acid of the base forming the cation and of the (super-) acid forming the anion influences the properties of the PIL. According to Miran et al.,[11] PILs with a high ΔpK_a value can achieve superior bulk properties, such as excellent thermal stability and high ionic conductivity. The concentration of the free base of the free acid in the protolysis equilibrium, as well as their volatilities, are

crucial parameters for (thermal) stability. The existence of non-ionic species and ion pairs reduces the proton activity and, respectively, the mobility.[12] However, PILs with a high ΔpK_a value are usually accompanied by very low cation acidity and are necessarily poor proton donators that can hardly deliver protons to the Pt surface necessary for the ORR. This will limit the ORR kinetics. However, it hardly seems possible to identify a single PIL that combines all of the desired properties, *i.e.*, high acidity, high proton conductivity, and high O_2 diffusivity/solubility (low polarity/hydrophilicity).

Therefore, the approach taken in this study is to combine the advantages of PILs with high and low ΔpK_a values by preparing blends with different compositions. The physico-chemical and electrochemical properties of the binary mixture are then investigated. The correlation between the physico-chemical properties, the interactions between the ions, and a resulting improvement in the electro-chemical properties is then discussed. The aim is the optimization of the properties of the bulk electrolyte and the Pt/PIL interface in order to gain a deeper understanding of electrochemical kinetics in non-aqueous electrolytes.

2. Experimental

In this study, blends of [2-Sema][TfO] and [Dema][TfO] were prepared and investigated. The chemical structure of these two PILs and the pK_a[13, 14] values of their cations and anions are shown in Fig. 1.

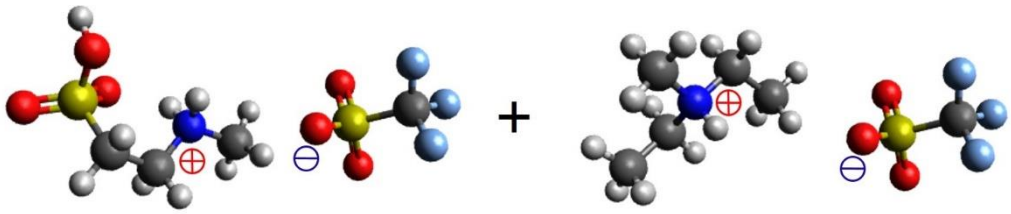

Figure 1. Structures of PIL cations and anions, pK_a values of the cations and, in the case of the anions, of the corresponding acid (TfOH).

2.1 Preparation of [2-Sema][TfO] and PILs mixtures of [2-Sema][TfO]/[Dema][TfO]

All substances were used as received. [2-Sema][TfO] was synthesized by slowly adding a stoichiometric amount of trifluoromethanesulfonic acid (reagent grade: 98%, Sigma Aldrich, USA) to 2-methylaminoethansulfonic acid (N-methyltaurine, ≥ 99 %, Sigma Life Sciences, USA) at 80 °C while stirring slowly. The mixture was then stirred at 80 °C for one hour. [Dema][TfO] (> 98 %, CAS No.: 945715-39-9, IoLiTec-Ionic Liquids Technologies GmbH, Germany) was used as received. The water content of [2-Sema][TfO] and [Dema][TfO] is 0.7 and 0.3 wt%, respectively, which was confirmed by means of Karl Fischer titration. For the preparation of the PIL blends with different molar ratios, [Dema][TfO] was slowly added to [2-Sema][TfO]. The mixtures were then stirred at 50 °C and sealed in a vessel in order to avoid the adsorption of water from ambient air.

2.2 Thermal gravimetric analysis (TGA)

The thermal stability of the PIL mixtures was determined using TGA (Perkin Elmer STA 6000). A small quantity of the samples (~10 mg) was dropped into quartz glass crucibles. The samples were heated from 100 to 500 °C at a heating rate of 10 °C min^{-1} under an N_2 atmosphere.

2.3 Electrochemical measurements

Measuring device, cells and electrodes:

The electrochemical measurements were performed using an impedance analyzer (“Zennium”, ZAHNER Elektrik GmbH, Germany). The in-house-designed measuring cell was described in detail in an earlier publication.[4] Two different, also in-house-designed working electrodes, were utilized for the different electrochemical measurements: i) a Pt wire (99.95%, Goodfellow GmbH, Germany) with a 1 mm Ø, fused in a glass tube with an open length of 6.8 mm; and ii) a Pt wire (99.9%, Heraeus) with 250 µm Ø, fully embedded in a soft glass tube (AG-Glas®, Schott AG, Germany) with a polished face side (micro-electrode).

A Pd wire (99.95%, Goodfellow GmbH, Germany) was also electrochemically-charged with H_2 for use as a reference electrode (Pd–H). All of the electrode potentials presented herein are plotted against Pd–H.

Polarization measurements (U/i)

The ORR polarization curves were recorded at a scan rate of 5 mV s^{-1} at 90 °C and with O_2 saturation. The starting potential was set to 1.1 V. The measurements were carried out using the Pt working electrode with 1 mm Ø.

Conductivity and viscosity measurements

The specific conductivities of the PIL mixtures were determined by utilizing the cell in a 2-electrode arrangement. The Pt wire with the 1 mm Ø was used as the working electrode and the Pt crucible as the counter electrode.[13] The cell constant was determined by using a 0.1 M KCl solution for calibration. The conductivities were measured from 60–120 °C, with temperature intervals of 10 °C. The corresponding viscosity of PIL mixtures was determined using viscometer (HAAKE MARS 60 Rheometers, Thermo Fischer Scientific Inc., USA).

Chronoamperometry measurements

The O_2 diffusion coefficient D_{O_2} and solubility c_{O_2} of the PIL mixtures were determined by means of chronoamperometry, using the 250 µm Ø circular Pt working electrode and O_2 saturation. The measurements were carried out by utilizing a procedure described by Mitsushima et al.[15]

3. Results and Discussion

3.1 Thermal Properties

The TGA curves of the [2-Sema][TfO]/[Dema][TfO] blends with different compositions are shown in Fig. 2. The decomposition temperature is defined as the temperature at which a weight loss of 5% occurs and is marked by the black dashed line in Fig. 2.

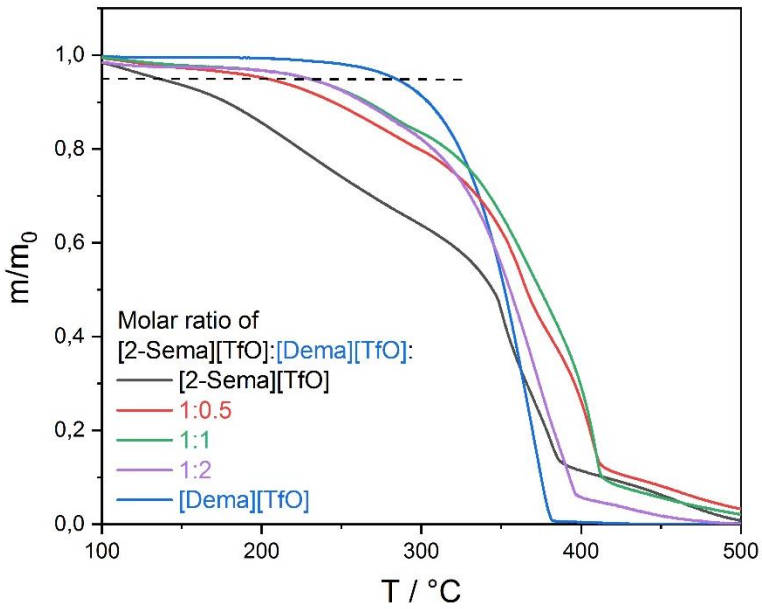

Figure 2. TGA curves of the PIL blends with different molar ratios. The heating rate is adjusted to 10 °C/min.

In the case of neat [2-Sema][TfO], a weight loss of 5% is exceeded at 127 °C, whereas [Dema][TfO] exhibits a higher decomposition temperature of 283 °C. By mixing [2-Sema][TfO] with [Dema][TfO], the thermal stability of the blend was significantly improved compared to neat [2-Sema][TfO]. The sample with a molar ratio of 1:2 exhibited the highest decomposition temperature of 228 °C (but only slightly higher than that of the 1:0.5 mixture). The significant increase in the decomposition temperature of about 100 °C is crucial, as a thermal stability beyond 200 °C is highly desirable when considering a PEMFC operating temperature of 100–120 °C.

The much lower thermal stability of [2-Sema][TfO] compared to [Dema][TfO] can mainly be attributed to the significantly smaller ΔpK_a value, *i.e.*, $\Delta pK_{a\,[2\text{-Sema}][TfO]} = 0.94–(-14.70) \approx 15.6$ *vs.* $\Delta pK_{a\,[Dema][TfO]} = 10.55–(-14.70) \approx 25.3$. It follows that for [2-Sema][TfO], the equilibrium of the proton exchange between the ions shifts more to the neutral compounds (here: *N*-methyltaurine and TfOH), as is the case for [Dema][TfO]:

$$CH_3NH_2^+(CH_2CH_2)SO_3\mathbf{H} + TfO^- \underset{k_2}{\overset{k_1}{\rightleftarrows}} CH_3NH_2^+(CH_2CH_2)SO_3^- + TfO\mathbf{H} \qquad (4)$$

This in turn means that a much higher concentration of volatile TfOH (T_b = 162 °C)[16] or TfOH hydrates are formed with residual water (*e.g.*, the monohydrate, T_b = 210 °C)[17] in [2-Sema][TfO] compared to [Dema][TfO]. *N*-methyltaurine is less volatile and decomposes at 247 °C.[18] In turn, the steady loss of volatile compounds will drag the reaction in Eq. (4) to the right side and, in the case of [2-Sema][TfO], results in considerable weight loss, even at 120 °C. For the above reasons, the enhancement of the thermal stability of the PIL blends can be explained by a thinning effect: the higher the amount of $[Dema]^+$ cations, the lower the molar fraction of $[2\text{-Sema}]^+$ cations and, according to Eq. (4), the lower the concentration of volatile TfOH and TfOH hydrates, respectively. FT–IR spectra confirm the varying molar fraction of the cations in the PIL blends (see Fig. S1 in the Supporting Information), exhibiting an overlay of the peaks of the neat PILs.

3.2 Specific Conductivity

The specific (total) conductivity σ of the PIL mixtures was determined in the temperature range of 60–120 °C, using temperature intervals of 10 °C. The Arrhenius plots of the specific (total) conductivities σ are depicted in Fig. 3. These exhibit a Vogel–Fulcher–Tamman (VFT) behavior, which can be described by the following equation:[4]

$$\sigma = \sigma_0 \, e^{-\frac{B_\sigma}{T-T_0}} \tag{7}$$

where σ_0 denotes the pre-exponential factor, B_σ the pseudo-activation energy of the specific conductivity, and T_0 the critical temperature. In viscous electrolytes, T_0 often correlates with the glass transition temperature T_g. The apparent (Arrhenius) activation energy E_a can be calculated as follows:[4]

$$E_a = RT + R\left(\frac{T}{T-T_0}\right)^2 B_\sigma \tag{8}$$

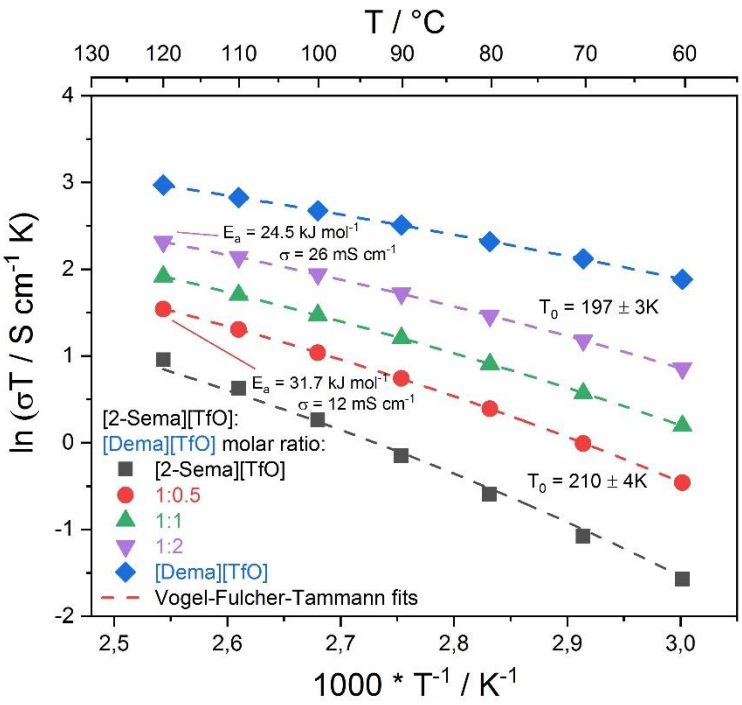

Figure 3. Arrhenius plots of the specific conductivities of PIL mixtures with different molar ratios at different temperatures. Inset picture: Viscosity of PIL mixtures with different molar ratios at 60 and 90 °C.

By blending [2-Sema][TfO] with [Dema][TfO], the (total) specific conductivity σ increases with a decreasing fraction of [2-Sema][TfO]. At 120 °C and a molar ratio of 1:2, a value of 25.7 mS cm^{-1} is reached, which is about four times higher than neat [2-Sema][TfO] (6.5 mS cm^{-1}). Because of the dominating vehicular proton transport in water-free PILs[19] and the above-mentioned, strong coupling of viscosity and ion transport, the significant increase in conductivity is primarily due to the strong decrease in viscosity when adding [Dema][TfO]. The viscosity of the sample with molar ratio of 1:1 decreased significantly from 0.22 to 0.08 Pa s at a temperature of 90 °C (see Fig. S2 in the Supporting Information).

The activation energy E_a and critical temperature T_0 of the neat PILs and PIL blends are compiled in Tab. 1. The activation energy E_a of the ionic transport is decreasing when blending [2-Sema][TfO] with [Dema][TfO]. Compared to neat [2-Sema][TfO], with an E_a of 37.2 kJ mol^{-1}, a mixture with a molar ratio of 1:0.5 exhibits a value of 31.7 kJ mol^{-1} and, in the case of a molar ratio of 1:2, a value of 24.5 kJ mol^{-1}. This

is a decrease of about 34% relative to neat [2-Sema][TfO]. The significant decrease of E_a and increase of σ, respectively, cannot be caused by a change in the proton transport mechanism. In anhydrous PILs, proton transport is based on a vehicle mechanism, as only the proton-carrying cations serve as mobile (vehicular) protonic charge carriers.[19] This should also apply to a blend of [2-Sema][TfO] with [Dema][TfO]. In addition to the neat PILs, in the blend, no interionic proton transfer processes are possible, as no amphoter such as water is present. In the case of a vehicular mechanism, due to the coupling of ionic and viscous transport, a lower viscosity will generally accelerate the ionic transport (Stokes–Einstein relation). Thus, the (total) conductivity σ and corresponding E_a of ILs and PILs are usually highly influenced by their viscosity.[4] [2-Sema][TfO] has a significantly higher viscosity compared to [Dema][TfO], and therefore blending [2-Sema][TfO] with [Dema][TfO] will strongly decrease the mixture's viscosity.

Table 1. Activation energy E_a and critical temperature T_0 of the neat PILs and PIL blends.

	[2-Sema][TfO]	blend 1:0.5	blend 1:1	blend 1:2	[Dema][TfO]
E_a / kJ mol^{-1}	37.2	31.7	28.8	24.5	20.0
T_0 / K	210	210	189	197	158

T_0 indicates the temperature, in which the free volume between the particles is assumed to be zero.[4] A critical temperature T_0 of 189 K for a 1:1 mixture is revealed by fitting a VFT model. This is about 20 K lower than the value found at 210 K for neat [2-Sema][TfO] and a 1:0.5 blend. The 1:2 blend exhibits a slightly higher critical temperature T_0 than the 1:1 mixture, but is still 10 K lower compared to neat [2-Sema][TfO]. Thus, the blends exhibit a higher fraction of free space for ion transport than neat [2-Sema][TfO] at the same temperature. A lower T_0 indicates weaker intramolecular force/less specific interionic interactions in the case of PIL blends, which may result in decreased viscosity in the PIL blends.

3.3 Oxygen Diffusion Coefficient D_{O_2} and Equilibrium Solubility c_{O_2}

The oxygen diffusion coefficient D_{O_2} and the equilibrium solubility c_{O_2} of the PIL blends were evaluated on the basis of the chronoamperometric data by applying the Shoup–Szabo equation.[20] As no limiting current density appeared in the case of the 1:2 mixture (see Fig. 5), a 1:0.75 mixture (≈ 43 mol% [Dema][TfO]) was used instead.

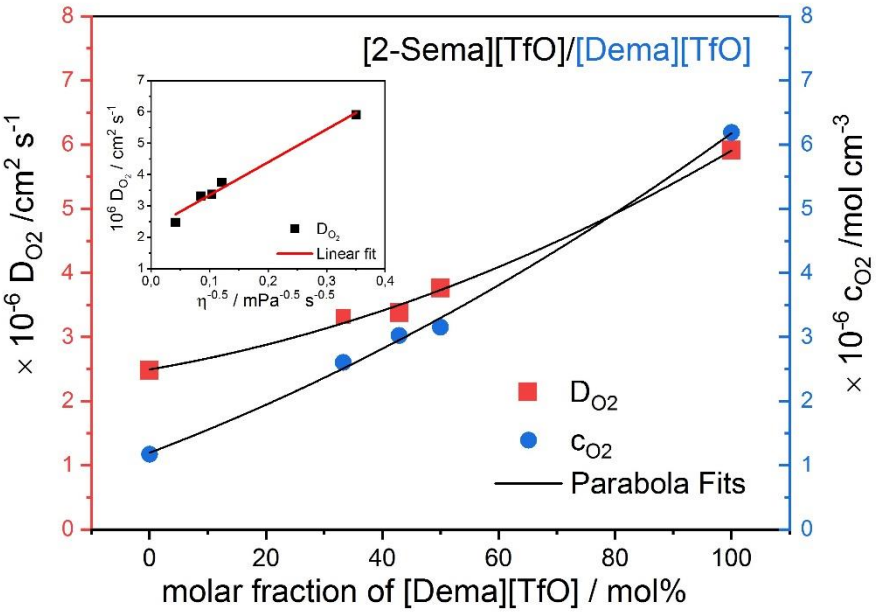

Figure 4. Oxygen diffusion coefficient D_{O_2} and equilibrium solubility c_{O_2} of the PIL blends at a temperature of 90 °C. Inset picture: Oxygen diffusion coefficient D_{O_2} as a function of the inverse square root of the viscosity of the PIL blends.[21, 22, 23]

As the less polar, less hygroscopic PIL, neat [Dema][TfO] exhibits, respectively, six and three times higher values for D_{O_2} and c_{O_2} compared to neat [2-Sema][TfO]. In the case of the PIL blends, D_{O_2} and c_{O_2} monotonically increase with an increasing fraction of [Dema][TfO], as depicted in Fig. 4. The blend with

the molar ratio of 1:1 features the highest value of $3.76 \cdot 10^{-6}$ cm^2 s^{-1} for D_{O_2} and of $3.15 \cdot 10^{-6}$ mol cm^{-3} for c_{O_2}.

As noted by Niedermeyer et al., a simple model for describing the thermodynamic properties of a mixture is, *e.g.*, the regular solution. In general, non-ideal behavior originates from the intermolecular interactions between the components; more specifically, if these interactions are stronger or weaker compared to those in the neat components, this will result in a non-zero mixing enthalpy $\Delta H_{mixture}$ and in activity coefficients for the components that differ from unity (ideal solution: $\Delta H_{mixture} = 0$).[24] For a PIL blend without specific interactions between the ions of the components (*e.g.*, ion pairs), a near ideal change in the properties of the ILs with the molar ratio of the mixture is expected.[25] However, different ion sizes in the PIL mixture can lead to a deviation from ideal behavior due to a change in the Coulombic interactions. As a result, a small, negative $\Delta H_{mixture}$ is observed.[26] Furthermore, Huang et al.[27] reported that the diffusivity of gas is reciprocal to the dynamic viscosity of the solution. More precisely, the diffusivity is approximately proportional to the inverse square root of the viscosity ($D_{O_2} \sim \eta^{-0.5}$).[28] In contrast, the simple Stokes–Einstein relationship ($D_{O_2} \sim \eta^{-1}$) is not valid in the case of the PILs and their mixtures. The inset picture in Fig. 4 confirms the proportionality of $D_{O_2} \sim \eta^{-0.5}$.[21, 22, 23] Therefore, the increasing diffusivity of oxygen in the PIL blends can be explained by the decrease in viscosity when adding [Dema][TfO] to [2-Sema][TfO]. Thus, the properties of the PIL blend is approximately an average of the bulk properties of [2-Sema][TfO] and [Dema][TfO].

3.4 Electrochemical Properties

Regarding the electrochemical activity in presence of PIL blends, the focus of this work is on the oxygen reduction reaction since the ORR at the PEFC cathode is still the bottleneck of the overall electrochemical process in PEM fuel cells. During the ORR process, changes in PIL stoichiometry nearby the electrode surface may take place. Taking as an example the neat anhydrous PIL, the BH^+ cation is the

proton donor in the ORR at the cathode side and an excess of B should be generated at the electrode surface. At the anode side protons are generated by the HOR, which will re-protonate the anion A^-, forming an excess of the acid HA. Thus, under fuel cell operation, a slight stoichiometry gradient regarding an excess of the base and the acid will be build up in the electrolyte. Finally, the neutral base B is re-protonated by the protons generated at the anode.

The current density *j* vs. cell potential *U* indicate the ORR kinetics and are shown in Fig. 5. The 1:0.5 and 1:1 PIL blends represent improved ORR kinetics compared to neat PILs, with [Dema][TfO] and [2-Sema][TfO] being in the potentially relevant range for fuel cell operation.

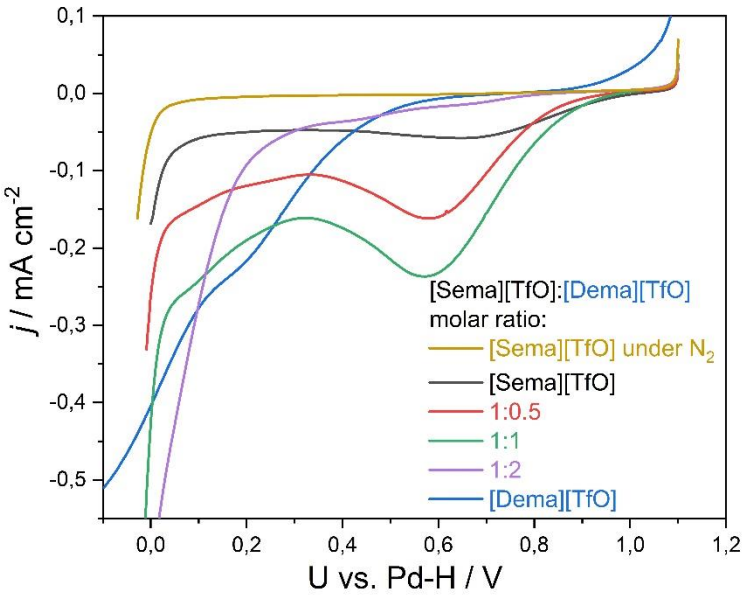

Figure 5. (Kinetic) ORR current density of a Pt electrode using the PIL blends, neat [2-Sema][TfO], or neat [Dema][TfO] (O_2 saturation, 90 °C and 5 mV/s). For comparison, the current density of [2-Sema][TfO] was also measured in the case of N_2 saturation (90 °C and 5 mV/s).

This can be attributed to the fact that at a temperature of 90 °C and O_2 saturation, neat [Dema][TfO] exhibits an ORR onset potential of 0.57 V, which means high overpotential of the ORR. Although it achieves a high limiting current density of about −0.73 mA cm^{-2} at −0.43 V, the diffusion limitation occurs at a fairly

high overpotential. Considering applications in fuel cells, this potential range is not relevant. Under the same conditions, neat [2-Sema][TfO] has a much more positive ORR onset potential of 0.93 V, *i.e.*, a much smaller overpotential of the ORR. However, the limiting current density of −0.05 mA cm^{-2} is smaller compared to neat [Dema][TfO] and already achieved at 0.7 V. The ratio of the limiting currents in presence of [Dema][TfO] and [2-Sema][TfO] (≈15, see Tab. 2) corresponds quite well with the ratio of the product of the oxygen solubility and oxygen diffusivity, that is 13 (see Fig. 4). The onset potential and corresponding limiting current density of neat PILs and PIL blends are shown in Tab. 2.

Table 2. ORR onset potentials and limiting current density j_{lim} of neat PILs and PIL blends at 90 °C.

	[2-Sema][TfO]	blend 1:0.5	blend 1:1	blend 1:2	[Dema][TfO]
Onset potential / V	0.93	0.88	0.92	0.71	0.57
j_{lim} / mA cm^{-2}	−0.05	−0.12	−0.19	–	−0.73

Clearly, the 1:0.5 and 1:1 PIL blends combine the favorable properties of both PILs, *i.e.*, the low ORR overpotential and high oxygen diffusion limiting current. In fact, adding [Dema][TfO] to [2-Sema][TfO] has two main effects: (*i*) a favorable increase in the limiting current occurs; and (*ii*) an unfavorable increase in ORR overpotential. Effect (*i*) is due to the much higher product $D_{O_2} \cdot c_{O_2}$ of [Dema][TfO] compared to [2-Sema][TfO] (see Section 3.3). Fortunately, effect (*ii*) is small if the amount of 50 mol% [Dema][TfO] is not exceeded. It can mainly be explained by the ten orders of magnitude lower acidity of the $[Dema]^+$ cation compared to the $[2\text{-Sema}]^+$ cation (pK_a of 10.55 *vs.* 0.94), which makes it a very poor proton donator for the ORR. In contrast, the $[2\text{-Sema}]^+$ cation turned out to be a fairly effective proton donator, thus enhancing the ORR rate constant and reducing the overpotential of the ORR.[10] A third (*iii*), minor effect is the approximately six times higher oxygen concentration in [Dema][TfO] compared to [2-Sema][TfO] (see Section 3.3) that will increase the ORR exchange current density and thus reduce the ORR overpotential.

However, this effect will probably be smaller than the above-mentioned, opposite effect caused by the poor proton-donating ability.

In the potential range between 0.2–0.8 V, the current densities of the PIL blends 1:0.5 and 1:1 are higher than those of the neat PILs, because effect (*i*) predominates and effect (*ii*) is small. Ultimately, effect (*ii*) is partially reduced by the third effect (*iii*). With a further increase in the amount of [Dema][TfO], the ORR current density significantly decreases, as effect (ii) dominates in the potential range of 0.3–1 V (see 1:2 mixture). Clearly, $[Dema]^+$ cations will replace $[2\text{-Sema}]^+$ cations near or on the Pt surface to a large extent. The substitution of a fairly effective proton donor ($[2\text{-Sema}]^+$) by a poor one ($[Dema]^+$) may explain the poor ORR performance, especially with high amounts of [Dema][TfO]. As a result of the aforementioned effects, the 1:1 mixture yields the highest ORR current densities in the application-relevant potential range. At the same time, the potential at which oxygen transport starts dominating the overall ORR process shifts to more negative values. The important effect is a significant extension of the applicable potential range in the 1:1 mixture compared to neat [2-Sema][TfO]. A deeper analysis of the ORR kinetics of the neat PILs and mixtures requires additional experiments, which are beyond the scope of this work, *e.g.*, measurements of the potential of zero charge (PZC) or the investigation of specific adsorbates on the electrode surface by means of *in situ* FT–IR or atomic force microscopy (AFM).

4. Conclusions

Binary PIL mixtures [2-Sema][TfO]/[Dema][TfO] exhibit outstanding bulk and electrochemical properties compared to neat [2-Sema][TfO], making them potential electrolytes for MT-PEMFC applications. In contrast, neat PILs are difficult to utilize as electrolytes in MT-PEM fuel cells: [Dema][TfO], for instance, exhibits insufficiently rapid ORR kinetics, leading to very poor ORR performance in the cathode potential range relevant for fuel cell operation, although it does exhibit high limiting current densities. [2-Sema][TfO] shows good ORR performance in the relevant potential range, but only low limiting current densities can be achieved. In the case of the neat PILs, the key properties that are often lacking include low diffusivity

and oxygen concentrations, limited proton conductivity, low thermal stability, and low proton donor abilities.

One approach for obtaining superior electrochemical performance is to blend PILs with different specific properties. It is essential that the following requirements be met: (a) The cation of one PIL must have high acidity. In the case of the presence of residual water, not only the cation itself will act as a good proton donator for the ORR but also H_3O^+ *via* the equilibrium between the cations and water molecules; and (b) a PIL that has fewer hydrogen bonds. As a result, the interaction between the ions is not very strong, which ensures a low viscosity and high conductivity of the PIL blend and, moreover, high diffusivity and solubility of the oxygen. The PIL blends investigated in this study feature improved bulk properties and enhanced electrochemical activity. By blending [2-Sema][TfO] and [Dema][TfO], the bulk and electrochemical properties of both PILs can be combined to a sufficient degree, *i.e.*, a better thermal stability (> 200 °C) and higher ORR current density (~4x) in the relevant potential range for fuel cell operation (0.8–1.0 V) compared to neat [2-Sema][TfO]. The decreased viscosity of the blend also leads to an increase in the total conductivity compared to neat [2-Sema][TfO]. Regarding the thermal stability, the PIL blends exhibit a slight, tolerable weight loss in the temperature range of 100-120°C. However, for operating temperatures much higher than 120°C, the thermal stability of the PIL mixtures is still an issue. In future works, the substitution of [2-Sema][TfO] by another acidic, but thermally more stable PIL such as [DESPA][TfO][29] would further increase the upper operation temperature limit. This would also decrease the release of TfOH during fuel cell operation.

The 1:1 mixture offers the best compromise between bulk electrolyte properties and ORR performance. The results may herald new opportunities for improving the bulk and electrochemical properties of PILs and so developing superior electrolytes for future MT-PEMFCs. This study helps to enlighten the rate limiting processes when using non-aqueous but protic electrolytes in fuel cells by performing basic investigations. It demonstrates a principle way to overcome the limitations given by the

specific properties of ionic liquid based electrolytes. It comes out that it is necessary to achieve not only a high oxygen diffusivity and solubility but also a sufficient donor activity to optimise the electrochemical performance in the technical relevant potential range.

Associated Content

Supporting Information

(a) FT–IR spectra of the PILs and PIL mixtures ([2-Sema][TfO]:[Dema][TfO]=1:0.5, 1:1, 1:2) at room temperature. (Figure S1).

(b) Viscosity of the PIL blends at temperatures of 60, 70, 80, 90 and 100 °C (Figure S2).

Conflicts of interest

There are no conflicts to declare.

Acknowledgements

We acknowledge Karl-Fischer titration of the electrolytes by K. Klafki. We are grateful to A. Schwaitzer (ZEA-1) for his preparation of the micro- and macroelectrodes. We are thankful to C. Wood for proofreading the manuscript.

References:

(1) Lei, Z.; Chen, B.; Koo, Y. M.; Macfarlane, D. R. Introduction: Ionic Liquids. *Chem. Rev.* **2017**, *117*, 6633–6635.

(2) Miran, M. S.; Hoque, M.; Yasuda, T.; Tsuzuki, S.; Ueno, K.; Watanabe, M. Key factor governing the physicochemical properties and extent of proton transfer in protic ionic liquids: ΔpK_a or chemical structure? *Phys. Chem. Chem. Phys.* **2019**, *21*, 418–426.

(3) Greaves, T. L.; Drummond, C. J. Protic ionic liquids: Properties and applications. *Chem. Rev.* **2008**, *108*, 206–237.

(4) Wippermann, K.; Wackerl, J.; Lehnert, W.; Huber, B.; Korte, C. 2-Sulfoethylammonium Trifluoromethanesulfonate as an Ionic Liquid for High Temperature PEM Fuel Cells. *J. Electrochem. Soc.* **2016**, *163*, F25–F37.

(5) Lee, J. S.; Nohira, T.; Hagiwara, R. Novel composite electrolyte membranes consisting of fluorohydrogenate ionic liquid and polymers for the unhumidified intermediate temperature fuel cell. *J. Power Sources* **2007**, *171*, 535–539.

(6) Wippermann, K.; Giffin, J.; Kuhri, S.; Lehnert, W.; Korte, C. The influence of water content in a proton-conducting ionic liquid on the double layer properties of the Pt/PIL interface. *Phys. Chem. Chem. Phys.* **2017**, *19*, 24706–24723.

(7) Lee, S. Y.; Ogawa, A.; Kanno, M.; Nakamoto, H.; Yasuda, T.; Watanabe, M. Nonhumidified intermediate temperature fuel cells using protic ionic liquids. *J. Am. Chem. Soc.* **2010**, *132*, 9764–9773.

(8) Technical data sheet (Diethylmethylammonium triflate), IoliTec-Ionic Liauids Technologies GmbH, 2015.

(9) Johnson, L.; Ejigu, A.; Licence, P.; Walsh, D. A. Hydrogen Oxidation and Oxygen Reduction at Platinum in Protic Ionic Liquids. *J. Phys. Chem. C* **2012**, *116*, 18048–18056.

(10) Wippermann, K.; Suo, Y.; Korte, C. Oxygen reduction reaction kinetics on Pt in mixtures of proton conducting ionic liquids (PILs) and water : Influence of the acidity of the cation. *J. Phys. Chem. C* **2021**, *125*, 4423–4435.

(11) Miran, M. S.; Yasuda, T.; Susan, M. A. B. H.; Dokko, K.; Watanabe, M.; Electrochemical properties of protic ionic liquids: Correlation between open circuit potential for H_2/O_2 cells under non-humidified conditions and ΔpK_a. *RSC Adv.* **2013**, *3*, 4141–4144.

(12) Miran, M. S.; Kinoshita, H.; Yasuda, T.; Susan, M. A. B. H.; Dokko, K.; Watanabe, M. Protic ionic liquids based on a super-strong base: Correlation between physicochemical properties and ΔpKa. *Mater. Res. Soc. Symp. Proc.* **2012**, *1473*, 1–6.

(13) Wippermann, K.; Giffin, J.; Korte, C. In Situ Determination of the Water Content of Ionic Liquids. *J. Electrochem. Soc.* **2018**, *165*, H263–H270.

(14) Trummal, A.; Lipping, L.; Kaljurand, I.; Koppel, I. A.; Leito, I. Acidity of Strong Acids in Water and Dimethyl Sulfoxide. *J. Phys. Chem. A* **2016**, *120*, 3663–3669.

(15) Mitsushima, S.; Shinohara, Y.; Matsuzawa, K.; Ota, K. I. Mass transportation in diethylmethylammonium trifluoromethanesulfonate for fuel cell applications. *Electrochim. Acta* **2010**, *55*, 6639–6644.

(16) Kazakova, A. N.; Vasilyev, A. V. Trifluoromethanesulfonic Acid in Organic Synthesis. *Russian Journal of Organic Chemistry* **2017**, *53*, 485–509.

(17) Hughes, V. B.; McNicol, B. D.; Andrew, M. R.; Jones, R. B.; Short, R. T. Electrolytes for methanol-air fuel cells. 11. The electro-oxidation of methanol in trifluoromethane-sulphonic acid monohydrate and aqueous solutions of trifluoromethane-sulphonic acid. *J. Appl. Electrochem.* **1977**, *7*, 161–174.

(18) Kalaitzis, J. A.; De Leone, P. A.; Quinn, R. J.; Healy, P. C. Zwitterionic 2-(methylamino)ethanesulfonic acid. *Acta Cryst.* **2003**, *E59*, o726–o727.

(19) Lin, J.; Korte, C. PBI-type Polymers and Acidic Proton Conducting Ionic Liquids – Conductivity and Molecular Interactions. *Fuel Cells* **2020**, *20*, 461–468.

(20) Shoup, D.; Szabo, A. Chronoamperometric current at finite disk electrodes. *J. Electroanal. Chem.* **1982**, *140*, 237–245.

(21) Yasuda, T.; Kinoshita, H.; Miran, M. S.; Tsuzuki, S.; Watanabe, M. Comparative study on physicochemical properties of protic ionic liquids based on allylammonium and propylammonium cations. *J. Chem. Eng. Data* **2013**, *58*, 2724–2732.

(22) Wippermann, K.; Suo, Y.; Korte, C. Suitability of the Hanging Meniscus RDE for the Electrochemical Investigation of Ionic Liquids. *J. Electrochem. Soc.* **2020**, *167*, 046511.

(23) Song, D.; Chen, J. Density and viscosity data for mixtures of ionic liquids with a common anion. *J. Chem. Eng. Data* **2014**, *59*, 257–262.

(24) Niedermeyer, H.; Hallett, J. P.; Villar-Garcia, I. J.; Hunt, P. A.; Welton, T. Mixtures of ionic liquids. *Chem. Soc. Rev.* **2012**, *41*, 7780–7802.

(25) Kleppa, O. J. The solution chemistry of simple fused salts. *Annu. Rev. Phys. Chem.* **1965**, *16*, 187-212.

(26) Kleppa, O. J.; Hersh, L. S. Heats of mixing in liquid alkali nitrate systems. *J. Chem. Phys.* **1961**, *34*, 351–358.

(27) Huango, X. J.; Rogers, E. I.; Hardacre, C.; Compton, R. G. The reduction of oxygen in various room temperature ionic liquids in the temperature range 293-318 K: Exploring the applicability of the Stokes-Einstein relationship in room temperature ionic liquids. *J. Phys. Chem. B* **2009**, *113*, 8953–8959.

(28) Condemarin, R.; Scovazzo, P. Gas permeabilities, solubilities, diffusivities, and diffusivity correlations for ammonium-based room temperature ionic liquids with comparison to imidazolium and phosphonium RTIL data. *Chem. Eng. J.* **2009**, *147*, 51–57.

(29) Hou, H.; Schütz, M.; Giffin, J.; Wippermann, K.; Gao, X.; Mariani, A.; Passerini, S.; Korte, C. Acidic ionic liquids enabling intermediate temperature operation fuel cells. *ACS Appl. Mater. Interfaces* **2021**, *13*, 8370-8382.